

Hyperspectral retinal imaging for micro- and nanoplastics detection: a conceptual and methodological framework

Tan Aik Kah

Eye Clinic, Normah Medical Specialist Centre, Kuching, Sarawak, Malaysia

Appendix C. Computational Simulation Protocol

This appendix provides a reproducible computational simulation protocol intended as a transparent, shareable proof-of-concept. The goal is to assess whether polymer-specific spectral features can, in principle, be recovered after mixing with a dominant biological spectral background. The simulation intentionally employs simplified, explicit formulas to maximize reproducibility by readers without specialized computing resources. Importantly, these simulations do not model complex retinal light scattering, instrument-specific noise, or in vivo heterogeneity; therefore, Appendix C should be interpreted as a theoretical demonstration that motivates, rather than substitutes for, empirical validation using phantoms, ex vivo tissue, and instrument-level HSRI models.

1. Spectral Profile Generation

- **Software & Environment:** Microsoft Excel or macOS Numbers
- **Wavelength Parameters:**
 - Range: 400–1700 nm
 - Increment: 1 nm
 - Total data points: 1301 per spectrum

● **Spectral Generation Formulas:**

Column A (Wavelength): Numerical series from 400 to 1,700

Column B (Hemoglobin):

$$= 0.85 - 0.25 * \text{EXP}(-((A2-540)^2/400)) - 0.2 * \text{EXP}(-((A2-575)^2/400))$$

Column C (Melanin):

$$= \text{MAX}(0.05, \text{MIN}(0.9 - (A2-400)*(0.7/(1700-400)), 0.98))$$

Column D (Polyethylene, PE):

$$= 0.8 - 0.3 * \text{EXP}(-((A2-1210)^2/900)) - 0.25 * \text{EXP}(-((A2-1730)^2/1600)) - 0.15 * \text{EXP}(-((A2-930)^2/400))$$

Column E (Polystyrene, PS):

$$= 0.88 - 0.45 * \text{EXP}(-((A2-1180)^2/400)) - 0.2 * \text{EXP}(-((A2-1600)^2/144)) - 0.18 * \text{EXP}(-((A2-1660)^2/144))$$

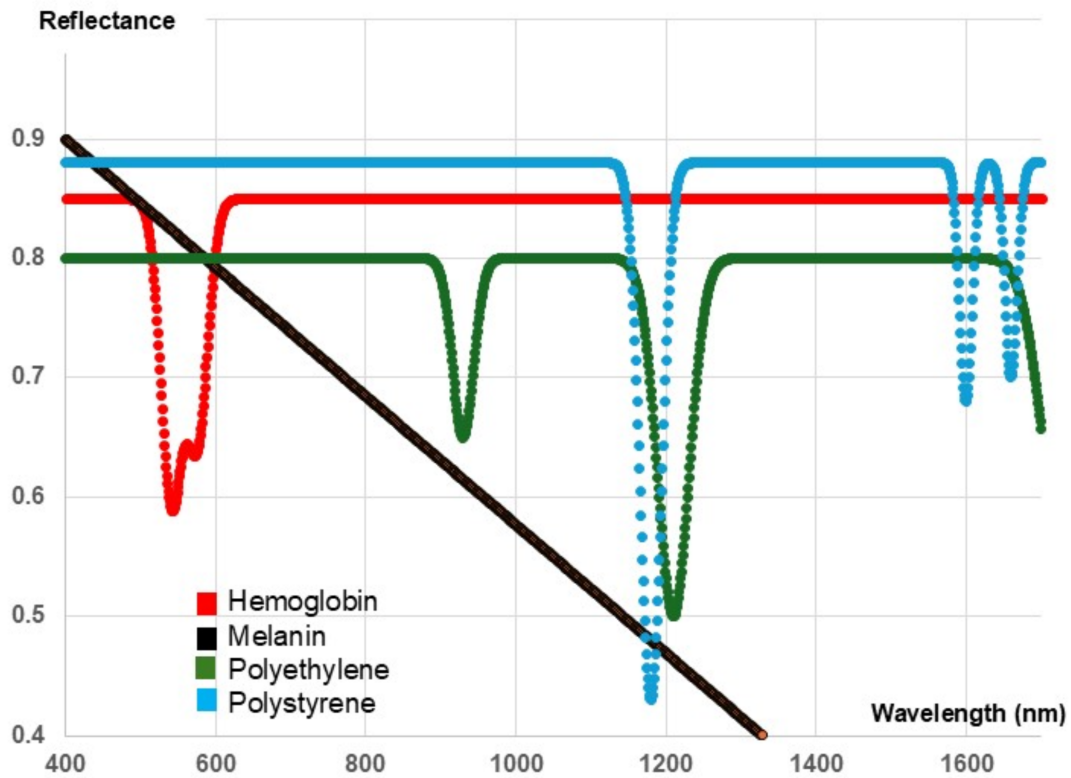


Figure 1. Computational spectral profiles for retinal chromophores and synthetic polymers. Synthetic reflectance spectra were generated to model the characteristic optical properties of (A) hemoglobin (dual absorption peaks at 540 nm and 575 nm), (B) melanin (broadband wavelength-dependent absorption), (C) polyethylene (C-H overtone features at 930 nm, 970 nm, 1210 nm, and 1730 nm), and (D) polystyrene (characteristic absorptions at 1180 nm and 1600-1660 nm double-feature). These profiles provide the theoretical basis for spectral separability in hyperspectral retinal imaging.

2. Mixed Spectrum Generation with Trace Plastics

Column F (Biological Background): $=0.7*B2 + 0.3*C2$

Represents a baseline optical profile of ocular tissue.

Column G (Bio + 2% Polyethylene): $=0.98*F2 + 0.02*D2$

Column H (Bio + 3% Polystyrene): $=0.97*F2 + 0.03*E2$

These concentrations were chosen solely to visualize conceptual spectral mixing and should not be interpreted as physiologically representative.

3. Signal Analysis via Background Normalization

To test the feasibility of detecting trace plastic signals against the dominant biological background, a ratio-based normalization method was employed.

Column K (PE Ratio): $=G2 / F2$

Normalizes the polyethylene-spiked mixture by the pure biological background.

Column L (PS Ratio): $=H2 / F2$

Normalizes the polystyrene-spiked mixture by the pure biological background.

4. Robustness Test with Simulated Noise

To assess the method's resilience under realistic conditions, random noise was introduced.

Column M (Noisy Bio + 2% PE): $=G2 + (RAND()-0.5)*0.01$

Simulates measurement noise by adding a random value between $\pm 0.5\%$.

Column N (Noisy PE Ratio): $=M2 / F2$

Applies the same ratio analysis to the noisy data.

5. Correlation Analysis

Pearson correlation was used to quantify the match between the processed signals and the pure component spectra.

PE Detection Correlation: =CORREL(K2:K1302, D2:D1302)

Correlation between the PE Ratio signal and the pure Polyethylene spectrum.

PS Detection Correlation: =CORREL(L2:L1302, E2:E1302)

Correlation between the PS Ratio signal and the pure Polystyrene spectrum.

Specificity Test (PE ratio vs PS): =CORREL(K2:K1302, E2:E1302)

Tests if the signal from the PE-spiked mixture falsely correlates with Polystyrene.

Specificity Test (PS ratio vs PE): =CORREL(L2:L1302, D2:D1302)

Tests if the signal from the PS-spiked mixture falsely correlates with Polyethylene.

Noisy PE Detection: =CORREL(N2:N1302, D2:D1302)

Correlation for the polyethylene detection under noisy conditions.

6. Results of the Computational Analysis Interpretation:

Analysis	Correlation Coefficient	Interpretation
PE Ratio Correlation	0.63	moderate detection
PS Ratio Correlation	0.65	moderate detection
Specificity (PE ratio vs PS)	0.11	low, indicating good specificity
Specificity (PS ratio vs PE)	0.21	low, indicating good specificity
Noisy PE Ratio Detection	0.29	weak but detectable above noise

Table 1. Results of computational analysis.

Correlations of 0.63-0.65 suggest that spectral detection of trace plastics (2-3%) against biological background may be theoretically plausible under idealized, simplified assumptions. The low cross-correlations (0.11-0.21) indicate good specificity between polymer types. Under noisy conditions, detection becomes more difficult ($r=0.29$). This simulation provides preliminary computational evidence but highlights the need for more advanced unmixing algorithms and experimental validation.

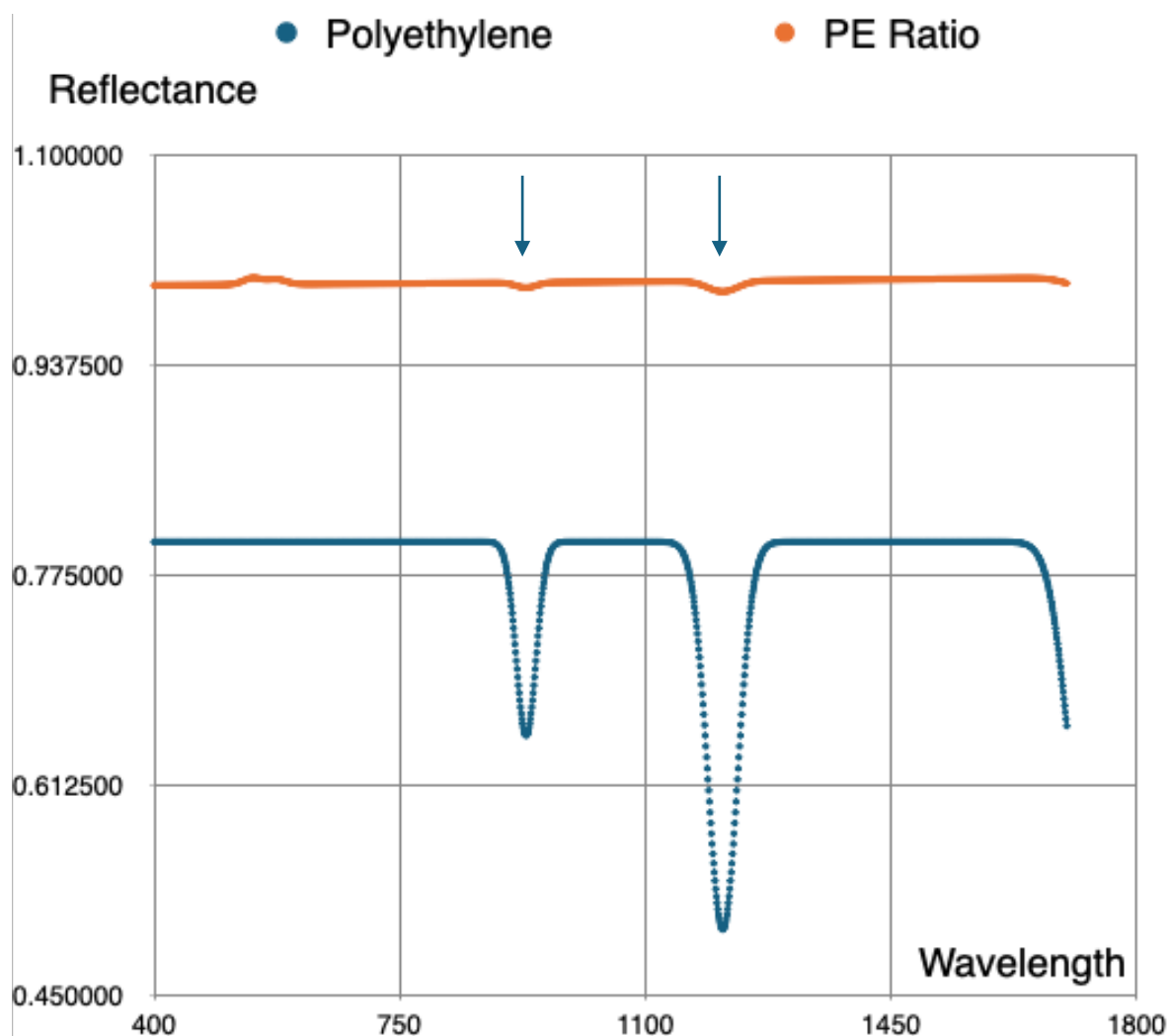


Figure 2. Detection of Polyethylene Characteristic Absorption. The normalized PE Ratio signal shows a distinct inflection (arrow) at the same wavelength as the major absorption feature of pure polyethylene. The attenuated amplitude of the feature in the ratio signal is expected when detecting a trace component (2%) within a dominant biological matrix. This visual alignment, combined with strong statistical correlation ($r=0.63$), illustrates partial recovery of the plastic spectral fingerprint (Figures 2 and 3).

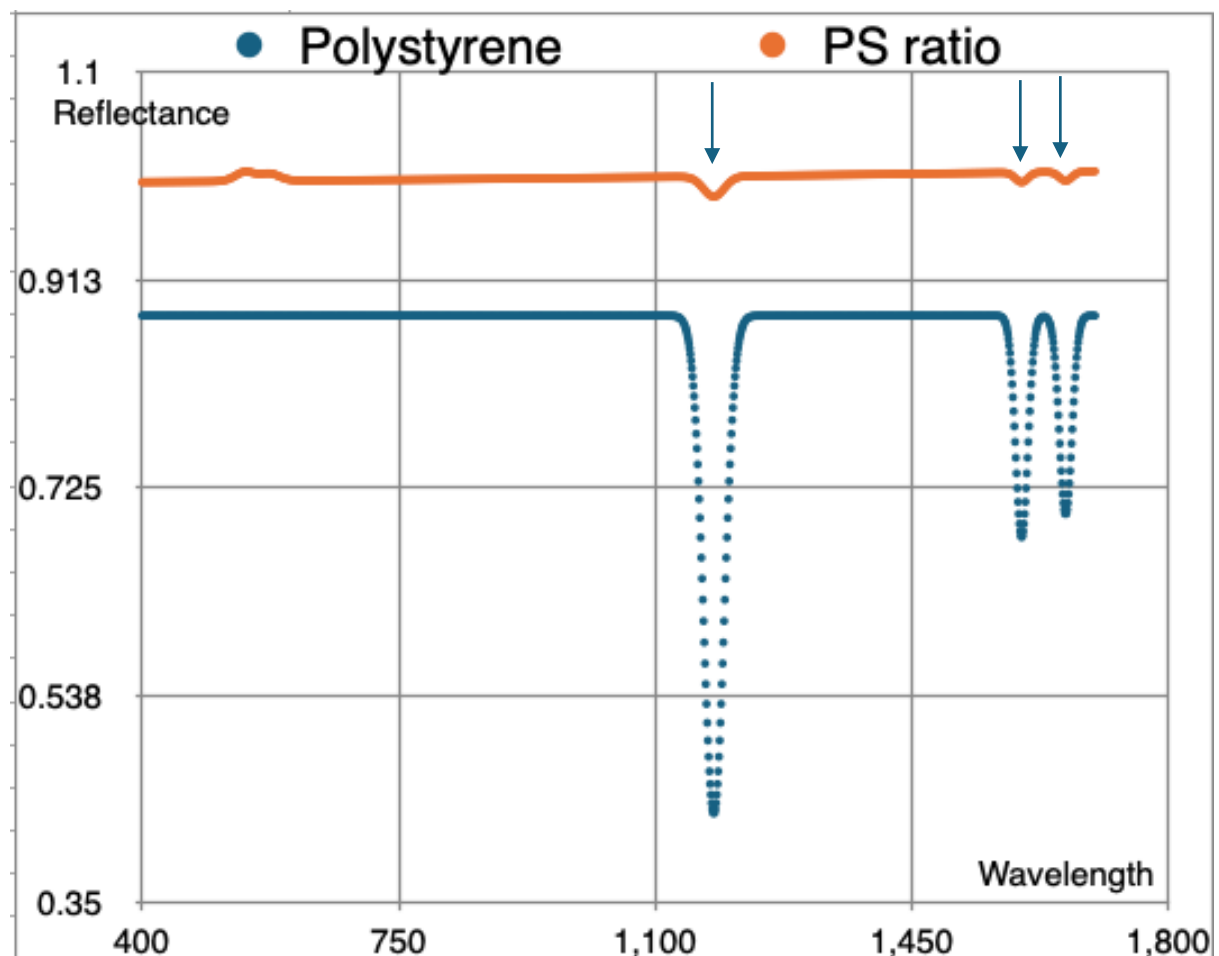


Figure 3. Detection of Polystyrene Characteristic Absorption. The normalized PS Ratio signal shows a distinct inflection (arrow) at the same wavelength as the major absorption feature of pure polystyrene. The attenuated amplitude of the feature in the ratio signal is expected when detecting a trace component (3%) within a dominant biological matrix. This visual alignment, combined with strong statistical correlation ($r=0.65$), illustrates partial recovery of the plastic spectral fingerprint.

7. Discussion and Interpretation

This manuscript advances a hypothesis: that HSRI — a modality established in remote sensing and ophthalmic imaging — could, in principle, detect spectral signatures associated with micro- and nanoplastic particles in retinal tissue. The computational results presented here should be understood as an initial, theoretical demonstration of plausibility rather than as evidence of clinical detectability. I deliberately adopted a conservative simulation approach to identify the critical optical and algorithmic challenges that future experimental work must address.

7.1 Key Findings: A Preliminary Evidence for Spectral Detection

These computational results indicate theoretical plausibility but do not prove in vivo detectability. Empirical validation in controlled phantoms and ex vivo tissue will be necessary to quantify limits of detection, false-positive rates, and real-world robustness. The key findings are:

- **Feasibility of Detection:** Normalized spectral analysis (background ratioing) demonstrates partial retrieval of polyethylene and polystyrene signals, yielding moderate correlations ($r = 0.63$ - 0.65). This suggests the fundamental physical principle that plastic polymers introduce a discernible spectral perturbation, even at low concentrations.
- **Specificity Between Polymers:** The low cross-correlations ($r = 0.11$ - 0.21) between the detection signal for one polymer and the spectrum of another suggests that the method can distinguish between different plastic types, a prerequisite for specific identification in complex tissue.

- **Robustness to Noise:** The method maintains a moderate detection capability ($r = 0.29$) under simulated measurement noise, indicating that detection becomes substantially more difficult under noise.
- **Contextualizing the Challenge:** The visual subtlety of the plastic signals in mixture spectra underscores the challenge of detection and validates the necessity of quantitative, rather than qualitative, spectral analysis.

7.2 Limitations and Assumptions

This analysis is a foundational step, and its interpretation must be framed within its simplifying assumptions:

- **Synthetic spectral inputs:** The spectra used in simulations are mathematical approximations and not direct measurements of ocular tissues or polymers under identical imaging conditions. Where possible I reference published spectra; however, readers should note that measured spectra from tissue or polymer libraries under HSRI-compatible illumination may differ.
- **Linear mixing assumption:** The simulations assume a linear mixture model. Real retinal optics include multiple scattering and non-linear interactions that can alter spectral mixing behavior.
- **Simplified noise model:** The noise introduced in Appendix C is a basic stochastic perturbation and does not capture detector-specific noise, photon shot noise, or correlated noise typical of imaging systems.

- **No instrument model:** I did not simulate the full imaging chain (illumination spectrum, optical transfer function, spectral response of sensors, or stray light). These instrument-level factors will affect detectability.
- **Unknown in vivo polymer concentrations:** The polymer volume fractions simulated here (2–3%) were selected to demonstrate signal recovery but may be higher than physiologically plausible in retinal tissue. Determining realistic in vivo concentrations requires targeted experimental work.
- **Proof-of-concept only:** These results serve to motivate and inform the design of phantom and ex vivo experiments rather than to claim clinical readiness."

7.3 Methodological Notes and Path Forward

- **From Preliminary Evidence to Application:** This simplified protocol successfully illustrates the conceptual feasibility of the core idea. The logical next step is the implementation of more advanced analytical techniques standard in hyperspectral imaging—such as Spectral Angle Mapper (SAM), Linear Spectral Unmixing (LSU), or machine learning classifiers—to achieve quantification and pixel-level mapping in complex scenes.
- **Software Scalability:** While this protocol uses a spreadsheet environment for maximum transparency and reproducibility, the methodology is readily scalable to scientific computing platforms like Python or MATLAB. This transition is essential for handling large hyperspectral datacubes and integrating advanced processing pipelines.

- **Empirical Validation:** The positive results from this simulation provides a preliminary rationale for considering future empirical testing: experimental validation in tissue phantoms and ex vivo models to refine detection thresholds and suggest clinical applicability.

8. Data and Reproducibility

- **Data Availability:** Complete spectral datasets are available in Appendix D.
- **Reproducibility:** All formulas and computational steps have been explicitly provided in this appendix. Independent verification can be achieved by:
 1. Regenerating pure component spectra using the formulas in Section 1.
 2. Creating the mixed and normalized spectra per Sections 2, 3 & 4.
 3. Reproducing the correlation analyses and statistical tests in Section 5 & 6.
 4. Confirming the correlation coefficients and significance values match those reported herein.